

ANALYSIS AND DESIGN OF WIDEBAND PLANAR YAGI- AND BI-YAGI ARRAYS WITH PHOTONIC BAND GAP

M. M. Abd-Elrazzak

Electronics & Communication Department, Faculty of Engineering
Almansoura University, Egypt

Abstract—In this work, the analysis and design of wideband microstrip yagi and bi-yagi antenna arrays with photonic band gap (PBG) is presented. By using the bi-yagi planar array, a high directive gain and a high front-to-back ratio are achieved in comparison with that of the single microstrip yagi structure. The current distribution, return loss, radiation pattern, and input impedance are calculated. For a single yagi, wide bandwidth up to 12.81% at 10.15 GHz is obtained. However, a high directive gain is achieved with the bi-yagi. The PBG structures force the antennas to have stop band at the higher end of the operating band. In addition, it increases the front-to back (F/B) ratio. The finite difference time domain (FDTD) with the perfect matched (PML) and a numerical package based on the method of moment (MOM) are used in the present analysis and design. A closed form based on an approximate equivalent circuit is used to get approximate dimensions of the PBG structures.

1. INTRODUCTION

During the last two decades, many literatures have been published for the design and optimization of planar microstrip antenna arrays [1–3]. In [1], multi-objective evolutionary algorithms (MOEAs) are used to optimize the yagi-antenna parameters to get specific antenna characteristics. A genetic algorithm is used in [2] for an optimum design of an asymmetric V-dipole antenna, and it is a three-element Yagi-Uda array. In addition, in [3] a modified two-element Yagi-Uda antenna with tunable beams in the H -plane (including four significant beams: forward backward, omni-directional, and bi-directional beams) is presented.

Recent papers have been presented [4, 5] for high gain yagi array antennas. In [4], two different long range yagi-Uda UHF RFID tag antennas have been designed and tested. The tag antenna size is reduced by using T-matching method. In [5], the effect of platform materials for high gain quasi-yagi planar antennas designed for mobile platform integration at 60 GHz is presented. High-gain compact stacked multilayered yagi antennas are proposed and demonstrated at 5.8 GHz for local positioning systems (LPS) applications [6].

In the present work, analysis and design are carried out for a wide band yagi and bi-yagi microstrip antenna arrays. The ground plane of the array is etched to produce photonic band gap (PBG) structures [7, 8]. These PBG structures are used to eliminate unrequired bandwidths at the higher end of the operating bandwidth and to increase the F/B ratio. The finite difference time domain (FDTD) with PLM [9–11] and a numerical package based on the method of moment (MOM) are used in the present analysis and design.

2. ANTENNA ARRAY STRUCTURES

In the present work, Fig. 1 and Fig. 2 show four different array structures which are the conventional microstrip yagi array, yagi with PBG, bi-yagi, and bi-yagi with PBG. The conventional microstrip yagi antenna array structure is shown in Fig. 1(a). It consists of seven patches with a strip feeder. These elements are classified into one rectangular driven element connected to the feeder, four square directors of length equal 15 mm, and two gap loaded reflectors. The dimensions of this structure are: $w_1 = 2$ mm, $w_2 = 24$ mm, $w_3 = 2$ mm, $w_4 = 18$ mm, $w_5 = 26$ mm, $L_1 = 2$ mm, $L_2 = 20$ mm, $L_3 = 15$ mm, $Lg_1 = Lg_2 = 4$ mm, $Lg_3 = 3$ mm.

The antenna is designed on a double copper (Cu) clad board of RT/duroid 5880 material ($\epsilon_r = 2.2$, $\tan \delta = 0.0009$ @ 10 GHz). The thickness of the substrate (h) is 1.5 mm. A low dielectric constant is used to get a small center-to center spacing between elements. This leads to decreasing the overall dimensions of the array. The feeder connected to the driven element is a microstrip line of a 50Ω which is suitable to be connected to the coaxial cable, or it can be transformed to a high impedance line through the use of a quarter-wave transformer.

A microstrip yagi array with PBG is obtained by etching 6-rectangular holes in the ground planes of length equal to 14 mm and width equal to 2 mm. The periodic distance (d) between the holes is taken equal to 6 mm (see Fig. 1(b)). The PBG structures are used to reduce the cross polarized radiation leading to increasing the antenna gain and directivity. In addition, the PBGs are used to eliminate the

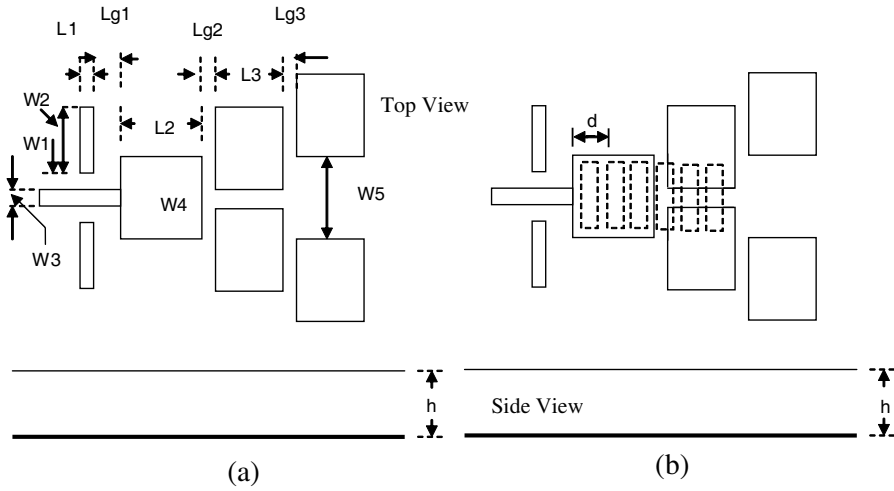


Figure 1. The top and side view of the yagi array. (a) The conventional yagi array. (b) The yagi array with PGB.

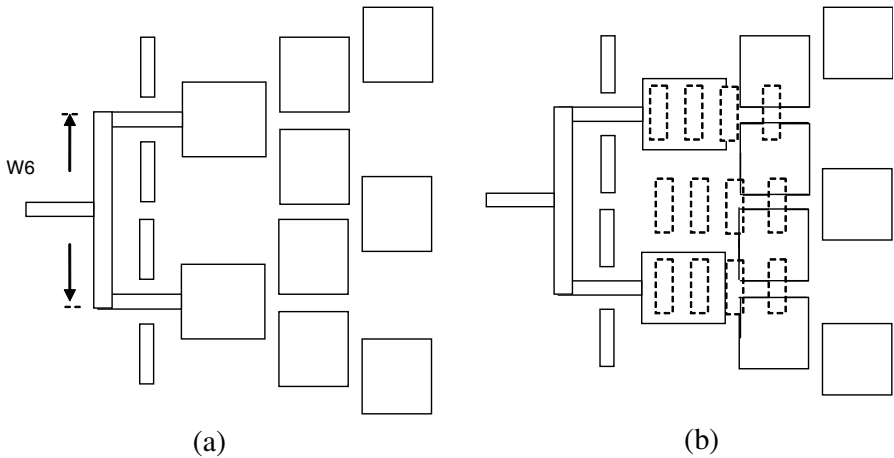


Figure 2. The top view of the bi-yagi array. (a) The conventional yagi array. (b) The yagi array with PGB.

pass bands at the higher end of the designed operating bandwidth.

The bi-yagi array is shown in Fig. 2 in which one director is used as a common director between the two arrays. The two arrays are fed in phase to allow increase in gain and directivity. The distance between the two yagi arrays is taken equal to $w_6 = 36$ mm. For the

bi-yagi array with PBG, three groups of PBG rectangular holes are etched in the ground plane. Each group consists of four rectangular holes of length 14 mm and width of 2 mm.

3. NUMERICAL RESULTS AND DISCUSSIONS

In this section, two different techniques are used for the analysis of the present structures. These techniques are the FDTD and a numerical package based on the method of moment (MOM). In addition, an approximate analytical formula based on an approximate equivalent circuit of the structures is used to determine the dimensions of the PBG [12]. The current distribution of the conventional yagi array is shown in Fig. 3. When PBG is added to the yagi array, a high current concentration is obtained on the driven, directors, and reflectors as shown in Fig. 4.

Figure 5 shows the return loss of the structures given in Fig. 1. The analysis is obtained using the FDTD and a numerical package based on the MOM. The results obtained by the two techniques are in good agreement. A wide bandwidth is obtained for the conventional yagi array where the center frequency is 10.15 GHz with BW of 12.81% at -10 dB. In addition, there is another band at a center frequency of 11.85 GHz with BW of 2.5%.

From Fig. 5, the use of PBG in the ground plane as discussed in section 2 leads to decreasing the bandwidth. At -10 dB, the BW is equal to 8.61% with center frequency of 10.45 GHz. However, it eliminates the passband at the higher end of the operating band as shown in the figure. This is carried out by choosing suitable periodic distance (d) between the rectangular PBG and the number of holes,

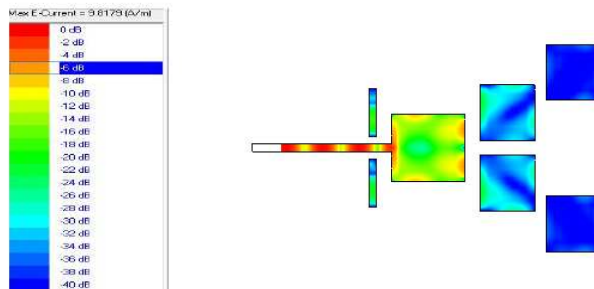


Figure 3. The current distribution of the conventional yagi shown in Fig. 1(a) at 11 GHz.

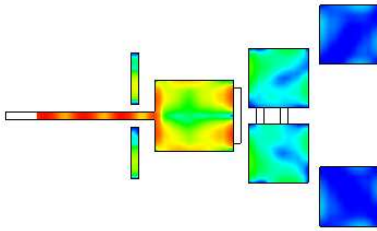


Figure 4. The current distribution of the yagi with PBG shown in Fig. 1(b) at 11 GHz.

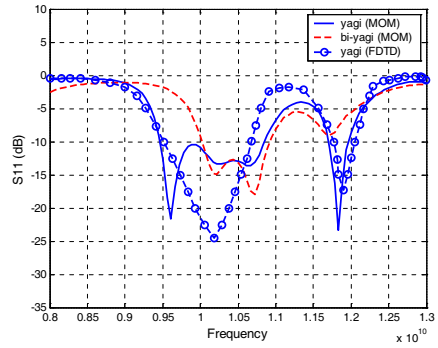


Figure 5. The scattering parameters of the conventional yagi and yagi with PBG shown in Fig. 1.

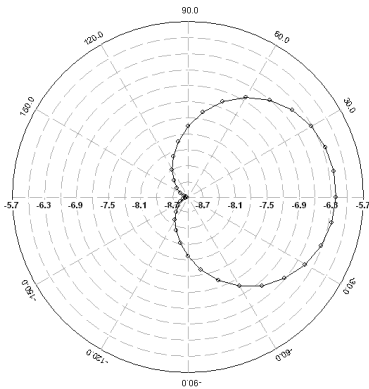


Figure 6. The radiation pattern of the conventional yagi shown in Fig. 1(a) at 10.5 GHz.

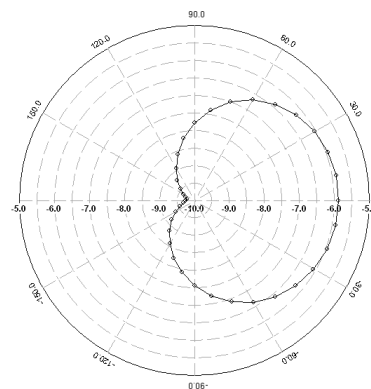


Figure 7. The radiation pattern of the yagi with PBG shown in Fig. 1(b) at 10.5 GHz.

and one can force the structures to have a stop band at 11.8 GHz. This is obtained using the following approximate formula:

$$f_o = \frac{\beta C}{2\pi\sqrt{\epsilon_{eff}}} \tag{1}$$

where,

$$\beta d = \pi/2,$$

and f_0 is the center frequency of the stop-band; ϵ_{eff} is the effective permittivity; and C is the speed of light in free space.

Figures 6 and 7 show that the use of the PBG leads to increasing the F/B ratio. The radiation pattern exhibits maximum radiation at 0° for the two cases in Fig. 6 and Fig. 7.

The input impedances of the yagi and yagi with PBG are shown in Fig. 8 and Fig. 9 where their real parts are equal to 50Ω in the operating frequency band, and its imaginary parts tends to be equal to zero.

Figure 10 shows the current distribution of the bi-yagi array given in Fig. 2(a). The two arrays are fed in phase which makes the current distribution symmetrical on the two arrays. The return losses of the bi-yagi and single yagi are shown in Fig. 11. The bi-yagi array exhibits a triple band response at 10.00 GHz, 11.51 GHz, and 12.75 GHz with

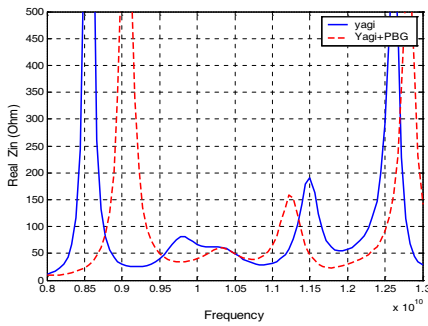


Figure 8. The real part of Z_{in} of the conventional yagi and yagi with PBG shown in Fig. 1.

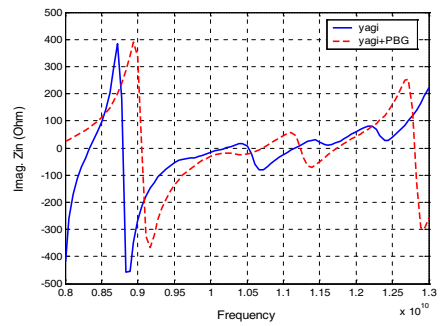


Figure 9. The imaginary part of Z_{in} of the conventional yagi and yagi with PBG shown in Fig. 1.

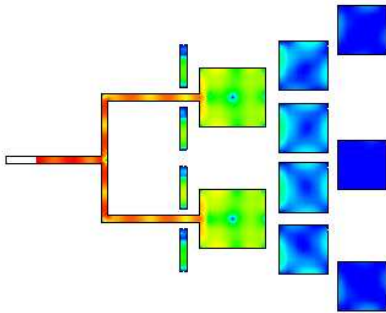


Figure 10. The current distribution of the bi-yagi shown in Fig. 2(a) at 10.08 GHz.

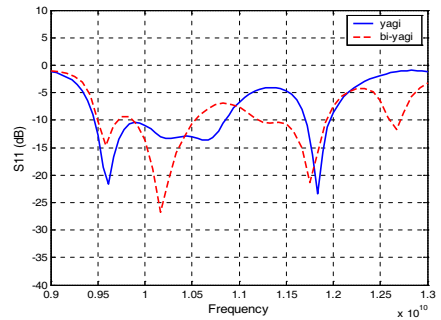


Figure 11. The scattering of the yagi and the bi-yagi shown in Fig. 1(a) and Fig. 2(a).

bandwidths equal to 10.00%, 5.21%, and 1.18%, respectively. The bandwidth of the first band of the bi-yagi is decreased compared with that of the yagi. However, the bi-yagi radiation pattern becomes more directive as shown in Fig. 12 than that of the yagi shown in Fig. 7. Fig. 13 shows the radiation pattern of the bi-yagi at 11.85 GHz where the direction of the maximum radiation is rotated at 70°.

The input impedance of the bi-yagi array is shown in Fig. 14 where it is equal to 50Ω in the operating frequency band while its imaginary part tends to be zero Ohm.

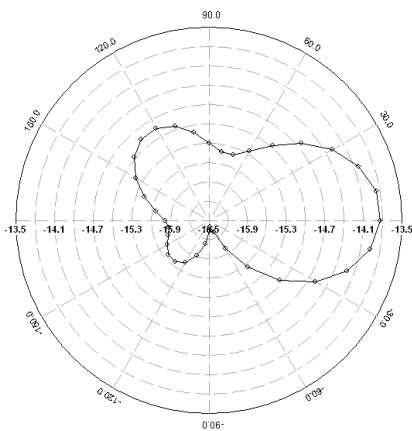


Figure 12. The radiation pattern of the bi-yagi shown in Fig. 2(a) at 10.08 GHz.

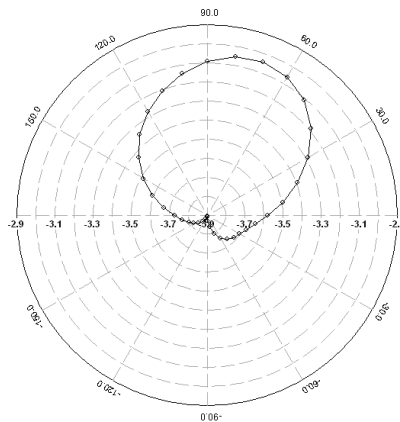


Figure 13. The radiation pattern of the bi-yagi shown in Fig. 2(a) at 11.85 GHz.

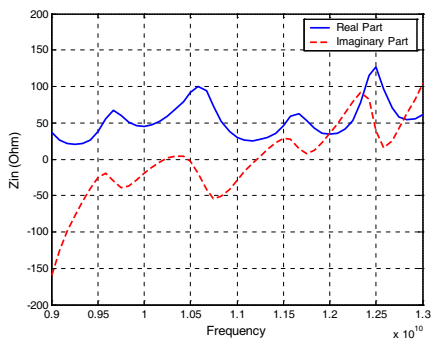


Figure 14. The input impedance of the bi-yagi shown in Fig. 2(a).

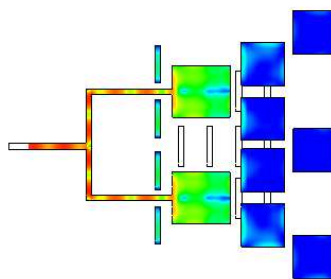


Figure 15. The current distribution of the bi-yagi with PBG shown in Fig. 2(b) at 10 GHz.

The current distribution of the bi-yagi array with PBG is shown in Fig. 15 in which the current is symmetrically distributed. The return loss of the bi-yagi with PBG and that of only bi-yagi are shown in Fig. 16. The bandwidth of the bi-yagi with PBG at -10 dB is increased compared with that of the first band of the bi-yagi array. In addition, the third band of the bi-yagi array is eliminated for the bi-yagi with PBG. This is because the PBG in the ground plane reduces the surface current and the cross polarized radiation of the array.

Figure 17 shows the radiation pattern of the bi-yagi array with PBG. This pattern becomes more directive than that of the yagi array without PBG (see Fig. 12). The input impedance of this array is shown

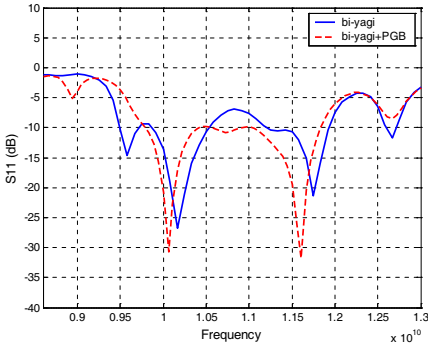


Figure 16. The scattering of the the bi-yagi and bi-yagi with PBG shown in Fig. 2.

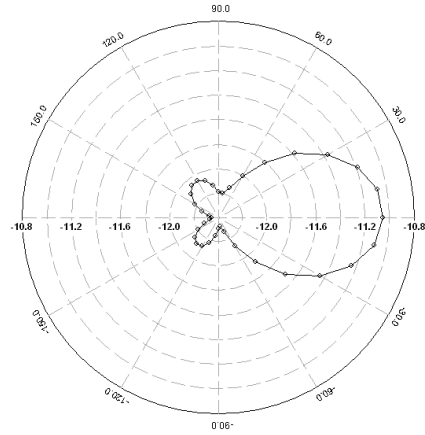


Figure 17. The radiation pattern of the bi-yagi with PBG shown in Fig. 2(b) at 10 GHz.

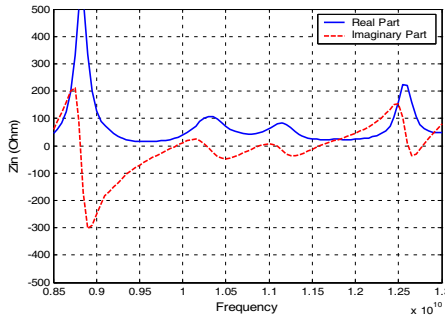


Figure 18. The input impedance of the bi-yagi with PBG shown in Fig. 2(b).

in Fig. 18. This impedance is almost real and equal to $50\ \Omega$ over the operating frequency band.

4. CONCLUSION

In this paper, the analysis and design of wideband microstrip yagi and bi-yagi antenna arrays with photonic band gap (PBG) are studied. By using the bi-yagi planar array, a high directive gain and with PBG a high front-to-back ratio are achieved in comparison with that of the single microstrip yagi structure. The current distribution, return loss, radiation pattern, and input impedance are calculated. For a single yagi, wide bandwidth up to 12.81% at 10.15 GHz is obtained. However, a high directive gain is achieved with the bi-yagi. The PBG structures force the antennas to have stop band at the higher end of the operating band. In addition, it increases the front-to back (F/B) ratio. The finite difference time domain (FDTD) with the perfect matched (PML) and a numerical package based on the method of moment (MOM) are used in the present analysis and design. A closed form based on an approximate equivalent circuit is used to get approximate dimensions of the PBG structures.

REFERENCES

1. Goudos, S. K., K. Siakavara, E. E. Vafiadis, and J. N. Sahalos, "Pareto optimal Yagi-Uda antenna design using multi-objective differential evaluation," *Progress In Electromagnetics Research*, Vol. 105, 231–251, 2010.
2. Misra, I. S. and R. S. Chakrabarty, "Design, analysis and optimization of V-dipole and its three-element Yagi-Uda array," *Progress In Electromagnetics Research*, Vol. 66, 137–156, 2006.
3. Sun, B. H., S.-G. Zhou, Y.-F. Wei, and Q.-Z. Liu, "Modified two-element Yagi-Uda antenna with tunable beams," *Progress In Electromagnetics Research*, Vol. 100, 175–187, 2010.
4. Lee, K. and Y. C. Chung, "High gain Yagi-Uda UHF RFID tag antennas," *Antenna and Propagation Society International Symposium*, 1753–1756, 2007.
5. Amadjikpè, A. L., G. E. Ponchak, and J. Papapolymerou, "High gain Quasi-Yagi planar antenna evaluation in platform material environment for 60 GHz wireless applications," *IEEE MTT-S International Microwave Symposium Digest, 2009, MTT'09*, 385–388, 2009.

6. Kramer, O., T. Djerafi, and K. Wu, "Vertically multilayer-stacked Yagi antenna with single and dual polarizations," *IEEE Trans. Antenna Propagat.*, Vol. 58, No. 4, 1022–1030, Apr. 2010.
7. Xiao, F., D. Yan, and Li Sun, "Optimization design of ground plane PBG structure of T-shape microstrip line by improved FGA," *International Conference on Microwave and Millimeter Wave Technology (ICMMT)*, 1561–1564, 2008.
8. Dahmardeh, M., A. Ghorbani, and A. Abdipour, "Active integrated antenna using photonic bandgap and defected ground structure," *3rd European Conference on Antenna and Propagation (EuCAP)*, 3823–3826, 2009.
9. Kuenz, K. S. and R. J. Luebbers, *The Finite-difference Time-domain Method for Electromagnetics*, CRC Press, London, Tokyo, 1993.
10. Tong, M. S., M. Yang, Y. Chen, and R. Mittra, "Finite difference time-domain analysis of a stacked dual-frequency microstrip planar inverted-F antenna for mobile telephone handset," *IEEE Trans. Antenna Propagat.*, Vol. 49, 367–376, Mar. 2001.
11. Yu, W., R. Mittra, and S. Chakravarty, "Stability characteristics of absorbing boundary conditions in microwave circuits simulations," *IEEE Trans. Antenna Propagat.*, Vol. 49, No. 9, Sep. 2001.
12. Baena, J. D., J. Bnache, F. Martin, R. Marques, F. Falcone, T. Lopetegi, M. A. G. Laso, J. Garcia-Garcia, I. Gil, M. Flores, and M. Sorolla, "Equivalent-circuit models for splitting resonators and complementry split ring resonators coupled to planar transmission lines," *IEEE Trans. Microw. Theory Tech.*, Vol. 53, No. 4, 1451–1461, Apr. 2005.